Neuro-Oncology 15(9):1173–1185, 2013.
doi:10.1093/neuonc/not065
Advance Access publication May 7, 2013

Intravenous injection of oncolytic picornavirus SVV-001 prolongs animal survival in a panel of primary tumor–based orthotopic xenograft mouse models of pediatric glioma

Zhigang Liu†, Xiumei Zhao†, Hua Mao, Patricia A. Baxter, Yulun Huang, Litian Yu, Lalita Wadhwa, Jack M. Su, Adekunle Adesina, Lazlo Perlaky, Mary Hurwitz, Neeraja Idamakanti, Seshidhar Reddy Police, Paul L. Hallenbeck, Richard L. Hurwitz, Ching C. Lau, Murali Chintagumpala, Susan M. Blaney, and Xiao-Nan Li

Diana Helis Henry Medical Research Foundation, New Orleans, LA (Z.L.); Laboratory of Molecular Neuro-oncology (X.Z., H.M., P.A.B., Y.H., L.Y., X.-N.L.); Texas Children's Cancer Center (X.Z., H.M., P.A.B., Y.H., L.Y., J.M.S., L.P., M.H., R.L.H., C.C.L., M.C., S.M.B., X.-N.L.); Center for Cell and Gene Therapy (L.W., M.H. R.L.H.); Department of Pathology (A.A.) , Texas Children's Hospital; Department of Pediatrics (P.A.B., J.M.S., A.A., L.P., M.H., R.L.H. C.C.L., M.C., S.M.B., X.-N. L.); Department of Ophthalmology (M.H., R.L.H.); Molecular and Cellular Biology (M.H., R.L.H.), Baylor College of Medicine, Houston, Texas (M.H., R.L.H.); Neotropix, Inc., Malvern, Pennsylvania, (N.I., S.R.P., P.L.H.)
Present Affiliations: State Key Laboratory of Oncology in Southern China, Department of Radiation Oncology, Sun Yat-sen University Cancer Center, Guangzhou 510060, China (Z.L.); Department of Ophthalmology, First Affiliated Hospital of Harbin Medical University, Harbin 150001, China (X.Z.)

Background. Seneca Valley virus (SVV-001) is a nonpathogenic oncolytic virus that can be systemically administered and can pass through the blood–brain barrier. We examined its therapeutic efficacy and the mechanism of tumor cell infection in pediatric malignant gliomas.
Methods. In vitro antitumor activities were examined in primary cultures, preformed neurospheres, and self-renewing glioma cells derived from 6 patient tumor orthotopic xenograft mouse models (1 anaplastic astrocytoma and 5 GBM). In vivo therapeutic efficacy was examined by systemic treatment of preformed xenografts in 3 permissive and 2 resistant models. The functional role of sialic acid in mediating SVV-001 infection was investigated using neuraminidase and lectins that cleave or competitively bind to linkage-specific sialic acids.
Results. SVV-001 at a multiplicity of infection of 0.5 to 25 replicated in and effectively killed primary cultures, preformed neurospheres, and self-renewing stemlike single glioma cells derived from 4 of the 6 glioma models in vitro. A single i.v. injection of SVV-001 (5×10^{12} viral particles/kg) led to the infection of orthotopic xenografts without harming normal mouse brain cells, resulting in significantly prolonged survival in all 3 permissive and 1 resistant mouse models ($P < .05$). Treatment with neuraminidase and competitive binding using lectins specific for α2,3-linked and/or α2,6-linked sialic acid significantly suppressed SVV-001 infectivity ($P < .01$).
Conclusion. SVV-001 possesses strong antitumor activity against pediatric malignant gliomas and utilizes α2,3-linked and α2,6-linked sialic acids as mediators of tumor cell infection. Our findings support the consideration of SVV-001 for clinical trials in children with malignant glioma.

Keywords: malignant glioma, oncolytic virus, orthotopic xenograft, SVV-001, sialic acid.

Glioblastoma multiforme (GBM) is the most malignant brain tumor that occurs both in children and in adults. Despite multimodality therapies, the median survival time in adult patients is only 12–18

Received June 18, 2012; accepted March 25, 2013.

†These authors contributed equally in this manuscript.

Corresponding Author: Xiao-Nan Li, MD, PhD, Texas Children's Cancer Center, Texas Children's Hospital, 6621 Fannin St, MC 3-3320, Houston, TX 77030 (xiaonan@bcm.edu).

months,[1] and 5-year survival in pediatric patients remains <20%.[2] Diffuse invasive growth and difficulties of effective drug delivery through the blood–brain barrier (BBB) are the challenges that have long been recognized in the treatment of malignant gliomas. Failure to eliminate cancer stem cells (CSCs), also referred to as tumor-initiating cells, might play a role in tumor recurrence,[3–5] but there are ongoing debates as to the relative abundance of CSC populations and the consistency of previously identified cell surface markers.[6,7] Since current treatments have proven ineffective in providing long-term survival, research on new therapeutic means of targeting malignant gliomas is of great importance.

Oncolytic viruses kill cancer cells through mechanisms different from conventional therapeutics; therefore, they may not be susceptible to the same pathways of drug or radiation resistance.[8–10] For childhood malignant gliomas, however, few studies have been reported, although multiple oncolytic viruses have exhibited antitumor activities against adult gliomas in vitro and/or in vivo.[11–19] Recently, several oncolytic viruses, including delta-24-RGD (arginine/glycine/aspartic acid) adenovirus, adenoviruses 16 and CV23, and oncolytic herpes simplex virus, were found to have potent therapeutic potential targeting adult glioma stem cells.[20–23] Although gene therapy for brain tumors has been found to be reasonably safe, efficient virus delivery into the brain still presents clinical challenges because many of the oncolytic viruses require direct intratumoral injection.[24,25] Therefore, viruses that can be systemically administered,[15,16,19,26] and new means of viral delivery,[24,27] are actively sought.

Seneca Valley virus (SVV)–001, also known as NTX-010, is a naturally occurring single-strand RNA virus that belongs to the family of *Picornaviridae*.[28–30] It is a nonpathogenic RNA virus that replicates only in the cytoplasm of host cells. SVV-001 has displayed antitumor activities in a spectrum of human cancer cells in established cell lines.[28,31] A recently completed phase I clinical trial confirmed that i.v. administration of SVV-001 was well tolerated at doses up to 10^{11} viral particles (vp)/kg, with predictable viral clearance kinetics, intratumoral viral replication, and evidence of antitumor activity in patients with small cell lung cancer.[32] One particularly attractive feature of SVV-001 for brain tumors is that SVV-001 can be administered through i.v. injection and pass through the BBB.[28,30,33]

We have recently demonstrated that a single i.v. injection of SVV-001 eliminated medulloblastoma xenograft tumors in vivo in mouse brains.[33] However, the effects of SVV-001 on pediatric malignant gliomas have not been thoroughly examined and little is known about the molecular mechanism(s) that determines the tropism of SVV-001. Previous virological studies indicate that binding to a target cell receptor is a critical initiating step in the virus life cycle.[34,35] A number of DNA and RNA viruses, including members of the *Picornaviridae* family,[36,37] have been shown to use sialic acids, which are often found at the terminus of the oligosaccharide attached to glycoproteins, glycolipids, or proteoglycans, as a component of their cellular receptor. Whether the infection of SVV-001 is mediated by sialic acids remains elusive to determine.

Limited availability of cell lines and animal models represents yet another major obstacle toward the development of new therapies for pediatric gliomas.[38] To overcome this barrier, we have developed a panel ($n = 6$) of orthotopic xenograft mouse models through direct injection of fresh surgical specimens of pediatric malignant gliomas into the brains of Rag2/Severe Combined Immunodeficient (SCID) mice. These xenograft tumors have since been strictly subtransplanted in vivo in mouse brains and are shown to have replicated the biology of the original patient tumors.[39] Using this unique panel as a clinically relevant model system, we examined the antitumor activities of SVV-001 in pediatric gliomas both in vitro and in vivo. Due to the heterogeneous nature of pediatric GBM, we also attempted to identify cell surface molecules that can potentially guide future identification of diagnostic markers to differentiate the permissive from the resistant tumors by determining whether sialic acid played any role in mediating SVV-001 infection.

Materials and Methods

The Viruses

SVV-001 (1×10^{14} vp/mL) and genetically engineered SVV-GFP (1×10^{12} vp/mL), which expresses green fluorescent protein (GFP), were obtained from Neotropix.[28] SVV-GFP has the identical tropism as the parent SVV-001 but with reduced cell lysis activities. The median tissue culture infectious dose of SVV-001—the amount of SVV-001 that will produce pathological changes in 50% of cell cultures on the permissive cell line (per.c6)—was 2.12×10^{12}/mL.[33] For in vitro treatment, SVV-001 and SVV-GFP were diluted into appropriate growth media, that is, serum-based Dulbecco's modified Eagle's medium for primary cultured cells and serum-free CSC growth medium containing human recombinant basic fibroblast growth factor (bFGF) and epidermal growth factor (EGF) (50 ng/mL each; R&D Systems) for the growth of neurospheres. For in vivo treatment, SVV-001 was diluted with phosphate buffered saline (PBS) and administered through a single tail vein injection.

Primary Tumor–based Orthotopic Xenograft Mouse Models

The Rag2 SCID mice were bred and housed in a specific pathogen-free animal facility at Texas Children's Hospital. All the experiments were conducted using a protocol approved by the Institutional Animal Care and Use Committee. Six transplantable orthotopic xenograft mouse models of pediatric glioma were included (Table 1). These models were established through direct injection of fresh surgical specimens into the right cerebrum (GBM, $n = 5$) or cerebellum (anaplastic astrocytoma, $n = 1$) of the Rag2/SCID mice and subtransplanted strictly in vivo in mouse brains following our surgical protocol described previously.[39] Briefly, tumor tissues

Table 1. List of the primary tumor–based orthotopic xenograft mouse models of pediatric gliomas

No.	Model ID	Age	Sex	Passages*	Permissive to SVV-001
1[39]	ICb-1227AA	16 y, 11 mo	F	8	Yes
2[39]	IC-1128GBM	8 y, 7 mo	M	8	No
3	IC-1406GBM	5 y	F	5	Yes
4	IC-1502GBM	4 y, 8 mo	F	4	No
5	IC-1621GBM	6 y	M	5	Yes
6	IC-2305GBM	9 y	F	5	Yes

Abbreviations: IC, intracerebral; ICb, intracerebellar; AA, anaplastic astrocytoma; GBM, glioblastoma multiforme. *Number of passages in vivo in mouse brains.

obtained from a cryostat laboratory were mechanically dissociated by 60 min of tumor removal. After the cell suspensions were passed through 35-micron cell strainers, the live tumor cells as single cells and small clumps (~5–10 cells) were counted with trypan blue staining. Tumor cells (1×10^5) were then suspended in 2 μL of culture medium and injected into mouse brains 1 mm to the right of the midline, 1.5 mm anterior (for intracerebral tumors) or posterior (for intracerebellar tumors) to the lambdoid suture, and 3 mm deep via a 10-μL 26-gauge Hamilton Gastight 1701 syringe needle. The animals were monitored daily until they developed signs of neurological deficit or became moribund, at which time they were killed. Characterization of the xenograft tumors showed that they replicated the histopathological, genetic, and invasive/metastatic features of patient tumors and preserved the $CD133^+$ glioma cells.[39]

Cell Viability and Cytotoxicity Assay

Primary cultured xenograft cells were seeded in 96-well plates in quadruplicates and treated with or without SVV-001 at a multiplicity of infection (MOI) of 0.5–25. Cell viability was checked with CCK-8, a "mix-and-measure" cell counting kit (Dojindo Molecular Technologies), as described previously.[40] To visualize viable tumor cells, 3-(4,5-dimethylthiazol-2-yl)-2,5-diphenyltetrazolium bromide was added to the culture medium 3 h before microscopy and photography.

Neurosphere Assay

Single-cell suspensions were plated in clonal density (1500 cells/100 μL) and incubated in CSC medium consisting of neurobasal media, N2 and B27 supplements (0.5× each; Invitrogen), human recombinant bFGF, and EGF (50 ng/mL each; R&D Systems).[39,41] Formation of neurospheres (>50 cells) was examined and neurospheres were counted under a Nikon phase-contrast microscope. To examine the infection of SVV-GFP preformed neurospheres, SVV-GFP (MOI = 20–2000) was added on day 14 and examined for expression of GFP in the following 1–7 days. To determine the cell killing effects of SVV-001 on self-renewing glioma stem cells, SVV-001 was added on day 1 of cell plating, and cell viabilities were quantitated with a CCK-8 assay (Dojindo) from day 3 to day 14.

In vitro Analysis of Viral Infection

Cells were seeded at 2000 per well in 96-well plates and cultured overnight. Following the addition of SVV-GFP at MOIs of 20, 200, and 2000, cells were imaged under fluorescence microscopy to detect the expression of GFP at 1, 7, 24, 48, and 72 h and at day 5. For flow cytometry analysis, the cells infected with MOIs of 20 and 2000 were harvested at 16, 24, 48, and 72 h and at day 7, washed twice, and resuspended in stem cell growth medium. Dead cells were excluded by propidium iodide staining (0.5 μg/mL). Side scatter and forward scatter profiles were used to eliminate cell doublets.

In vivo Treatment

SVV-001 (5×10^{12} vp/kg) was diluted with PBS and administered through a single tail vein injection in 5 GBM mouse models at 2 and 4 weeks ($n = 10$) after tumor injection. Body weights were monitored weekly as a surrogate indicator of SVV-001 systemic side effects. Mice that developed neurological deficits were killed and their whole brains removed for histopathological analysis. Mice receiving PBS only ($n = 10$) were included as controls. To study the biological changes caused by SVV-001, we allowed the injected xenograft cells in a separate group to grow for ~8 weeks to form tumors 8–10 mm in diameter before being treated with SVV-001 as described. Mouse brains were then removed at 1, 2, 4, and 7 days ($n = 2–3$ per time points) after virus injection and examined.

Immunohistochemical Staining

Immunohistochemical (IHC) staining was performed using a Vectastain Elite kit (Vector Laboratories) as we described previously.[42] Primary antibodies included mouse monoclonal antibodies against SVV-001 capsid protein (2A9, 1 : 200; Neotropix) and human-specific mitochondria (1 : 50; Abcam). Antigen retrieval was performed in a pressure cooker in 0.03-M sodium citrate acid buffer. After slides were incubated with primary antibodies, the appropriate biotinylated secondary antibodies (1 : 200) were applied, and the final signal was developed using the 3,3′-diaminobenzidine substrate kit for peroxidase.

Western Blotting

Proteins from untreated xenograft tumors were extracted with Trizol, separated with NuPAGE Novex Bis-Tris 4%–12% gel (Invitrogen), and transferred to polyvinylidene fluoride membranes (Bio-Rad). Detection of sialic acids was performed using biotinylated lectins that bind to specific linkage in sialic acid, including *Maackia amurensis* lectin (MAL), which binds to α2,3-linked sialic

acid, and *Sambucus nigra* lectin (SNL), which binds to α2,6-linked sialic acid. Polyvinylidene fluoride membranes were blocked with Carbo-Free Blocking Solution (Vector Laboratories) and incubated with biotinylated lectins (10 μg/mL) for 30 min at room temperature. Sialic acids were visualized by electrochemiluminescence using an ECL Plus Western blotting detection system (Amersham Biosciences). For loading control, anti–β-actin antibodies (1 : 2000; Sigma) were used.

Treatment of Glioma Cells With Neuraminidases

Freshly harvested glioma xenograft cells were incubated overnight at 37°C before being treated with neuraminidase from *Vibrio cholerae* (Sigma-Aldrich), ranging from 3.125 mU/mL to 25 mU/mL for 60 min. Neuraminidase cleaves α2,3-linked and α2,6-linked terminal sialic acid residues and α2,8-linked internal sialic acid residues. Cells were then washed 3 times, and cell viability and SVV-GFP infectivity assays were carried out as described.

Competitive Inhibition of SVV-GFP Infectivity by Lectins

Competition was done using 3 lectins that have been shown to bind to specific linkage in sialic acid, including MAL, which binds to α2,3-linked sialic acid; SNL, which binds to α2,6-linked sialic acid; and *Trichomonas mobilensis* lectin (TRI; Sigma-Aldrich), which binds to both α2,3- and α2,6-linked sialic acids. A total of 10^5 cells were preincubated with MAL, SNL, and TRI at concentrations of 0 mg/mL, 0.05 mg/mL, and 0.1 mg/mL in 0.1 mL of PBS on ice for 1 hr, followed by exposure to SVV-GFP (MOI = 2000) on ice for an additional 1 h. The treated and untreated cells were then washed 3 times with PBS to remove lectins and SVV-GFP viruses. After the cells were incubated for 48 h, they were harvested and the percentage of GFP^+ cells determined by flow cytometry.

Statistical Analysis

In vitro cytotoxic effects and changes of SVV-GFP infectivity were analyzed through a 1-way ANOVA followed by pairwise comparison using the Tukey method; differences in animal survival times were analyzed with a log-rank analysis using SigmaStat (Systat Software). The data were graphed with SigmaPlot (Systat Software).

Results

SVV-001 Kills Primary Cultured Glioma Xenograft Cells In vitro

To determine the antitumor activities of SVV-001 against pediatric gliomas, we incubated freshly isolated glioma xenograft cells in vitro in the presence of SVV-001 (MOI = 0.5–25). Since SVV-001 is a naturally occurring virus and is the first member of a new genus called Senecavirus in the family of *Picornaviridae*,[28,43] there is currently no other virus that can be included as an appropriate mock virus. The untreated cells were therefore included as controls. A 72-h treatment with SVV-001 at MOI = 0.5 resulted in significant cell killing in 4/6 models (66.7%), causing more than 90% cell death in 3 mouse models (ICb-1227AA, IC-1406GBM, and IC-1621GBM), and more than 85% cell death in mouse model IC-2305GBM ($P < .01$). Tumor cells from the 2 remaining mouse models (IC-1502GBM and IC-1128GBM) were resistant to SVV-001 even at MOI = 25 (Fig. 1A).

SVV-001 Infects GBM Cells in the Preformed Neurospheres

Since CSCs are shown to be drug resistant and may represent the seed cells that cause tumor recurrence,[3] we next examined whether SVV-001 could overcome the defense mechanisms and exert efficient infection of glioma stem cells. Recognizing that the commonly used glioma stem cell markers, CD133 and CD15, may not identify all the glioma stem cells,[6] we utilized the neurosphere assay, a functional assay that reliably defines the self-renewal capacity of CSCs in vitro,[44] to examine whether glioma neurospheres could be efficiently infected by SVV-GFP. Since the genetically engineered SVV-GFP maintained identical tropism but with reduced oncolytic activities compared with the parent SVV-001, higher MOIs were applied. Preformed neurospheres derived from 4 permissive and 2 resistant mouse models were treated with SVV-GFP at MOIs of 20, 200, and 2000 for 7 days and compared with those of the control cells through time-course microscopic and flow cytometric examination of GFP expression, which is indicative of intracellular replication of SVV-GFP. In the 4 permissive models, infection of their neurosphere cells was observed as early as 24 h, and the increase of GFP^+ cells was both time- and dose-dependent (Fig. 1B and C). The 4 mouse models, however, did not respond equally to the SVV-GFP infection. The highest levels of GFP^+ cells were observed on day 3 in ICb-1227AA (~15%), on day 2 in IC-1406GBM (~75%) and IC-1621GBM (~30%), and on day 1 in IC-2305GBM (~4%). Parallel to increased GFP positivity, there was a rise of doubly positive cells (propidium iodide and GFP; Fig. 1B), indicating that cell death was also increased after exposure to SVV-GFP viruses. In the 2 resistant mouse models, no intracellular expression of SVV-GFP was detected (Fig. 1C). These data suggest that SVV-GFP could overcome the defense mechanisms of GBM neurospheres in the permissive GBM mouse models, whereas in the resistant models the lack of intracellular replication of SVV-GFP suggests that SVV-GFP was either not able to get into the cells, or not able to replicate inside the GBM cells, or both.

SVV-001 Targets Self-renewing Glioma Stem Cells In vitro

To further determine whether SVV-001 could kill GBM cells capable of forming neurospheres in vitro, we plated freshly isolated single GBM cells at clonal density (2000 cells/0.1 mL) in serum-free medium supplemented

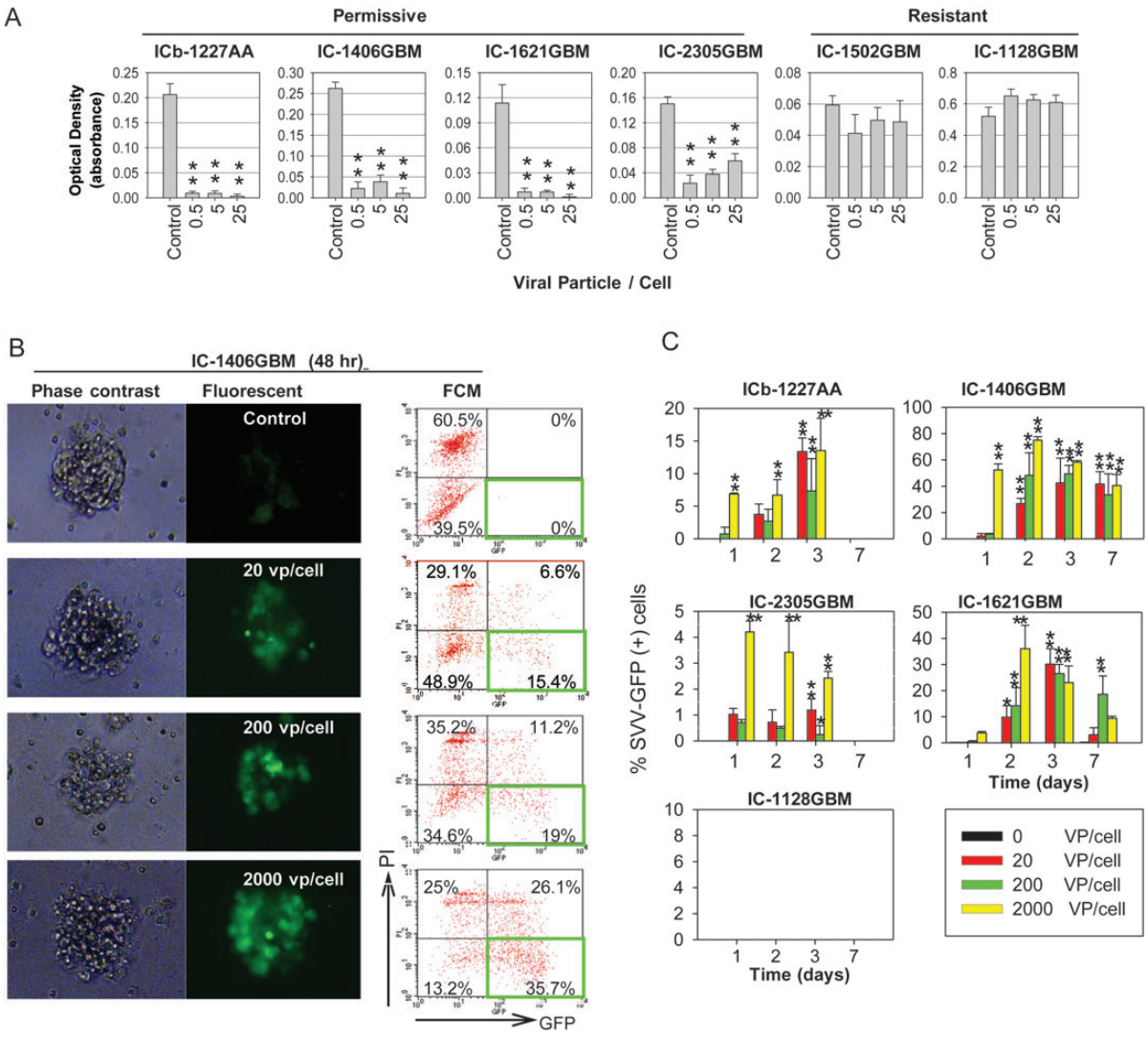

Fig. 1. Effects of SVV-001 on primary cultured tumor cells and preformed neurospheres derived from GBM xenograft models. **(A)** Killing of primary cultured GBM xenograft tumor cells by SVV-001. Cell viability was estimated using CCK-8 assay by measuring the absorbance at 460 nm after the cells were exposed to SVV-001 ranging from 0 to 25 vp/cell for 72 h. $^{**}P < .01$ compared with the untreated control. **(B)** Infection of preformed GBM neurospheres with SVV-GFP. Representative images (left panel) and flow cytometry (FCM) quantitative analysis (right panel) of viable GFP^+ cells (right lower quadrant) as well as dead GFP^+ cells (right upper quadrant) in neurospheres derived from IC-1406GBM 48 h post incubation with SVV-GFP, ranging from 0 to 2000 vp/cell. **(C)** Graphs showing the time-course analysis of SVV-GFP infection in the permissive models (ICb-1227AA, IC-1406GBM, IC-2305GBM, and IC-1621GBM) as examined through FCM analysis of GFP^+ cells ($^{*}P < .05$, $^{**}P < .01$). By day 7, the GFP^+ cells in ICb-1227AA and IC-2305GBM became undetectable. No GFP expression was detected in the resistant model IC-1128GBM.

with EGF and bFGF, which is shown to favor the growth of glioma stem cells,[5] and treated them with SVV-001 at MOI = 0.5–25 for 14 days. Time-course analysis of cell viability showed that SVV-001 nearly eliminated the growth of the self-renewing GBM cells starting from day 3 at MOI = 5 in ICb-1227AA and at MOI = 0.5 in IC-1406GBM ($P < .01$; Fig. 2). In these 2 mouse models, prolonged incubation until day 14 did not yield the formation of new neurospheres, indicating the absence of cells resistant to SVV-001. Significant suppression of neurosphere growth was also observed in the third mouse model, IC-1621GBM (>70% at day 3 at MOI = 5). In the fourth model, IC-2305GBM, however, although >80% suppression was observed at days 3 and 7 at MOI = 0.5 ($P < .01$), some of the treated cells were still proliferating, albeit at a slower rate than the untreated control, until day 14, suggesting that there existed a subpopulation of SVV-001–resistant cells in this model (Fig. 2). In the 2 resistant models, SVV-001 failed to cause any suppression of neurosphere formation.

Systemically Administered SVV-001 Can Infect Intracranial Glioma Xenograft Tumors

One of the advantages of SVV-001 relative to many other oncolytic viruses is that it can be administered through

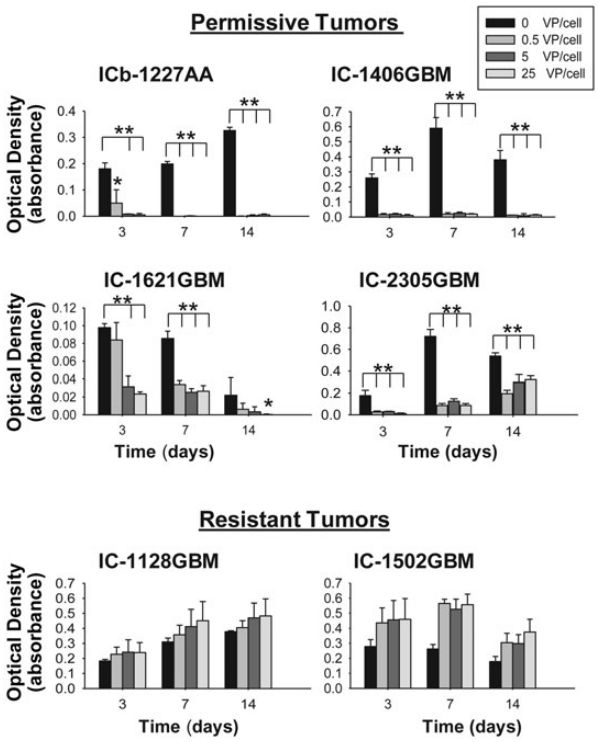

Fig. 2. Growth suppression of self-renewing single GBM cells by SVV-001 in vitro. Single GBM cells were plated in clonal density in quadruplicates in 96-well plates and incubated in serum-free medium containing growth factors (EGF and bFGF) that favor the growth of CSCs. Formation of neurospheres was examined under a phase-contrast microscope, and cell viability was examined with a CCK-8 assay. *$P < .05$, **$P < .01$ compared with untreated control.

i.v. injection,[33] as it is not inactivated by components of human blood.[28] To determine whether SVV-001 could also pass through the BBB and effectively infect GBM xenograft cells in mouse brains, we administered SVV-001 (5×10^{12} vp/kg) through a single tail vein injection into the mice bearing relatively large intracerebral xenograft tumors (8–10 wk post tumor cell engraftment). The time-course infection of tumor cells was examined in 3 permissive GBM models through IHC detection of the capsid protein of mature SVV-001 viruses and compared with the 2 resistant models. In 2/3 of the permissive models (ICb-1227AA and IC-1406GBM), isolated positive cells could be seen as early as 24 h post viral injection (Fig. 3A, a). By 48 h, positive cells could be seen in all 3 permissive models, and some of them formed small clustered patches (~20 cells at cross section) (Fig. 3A, b). These clustered cells increased to form larger areas of positive cells (several hundred at cross section) by 96 hr, in which the cytoplasm was filled with strong positive reactions (Fig. 3A, c). Many cell nuclei became condensed or fragmented, indicative of cell lysis as well. In addition to tumor cells in the core area, single cells in the invasive front, particularly in ICb-1227AA, were also found to be infected (Fig. 3B, i–k). By day 7, the SVV-001–positive areas increased remarkably (Fig. 3A, d). These results showed that SVV-001 could pass through the BBB, although it is still controversial whether the GBM xenograft tumors have the intact BBBs, and effectively infect GBM xenograft tumors in a time-dependent manner. In the resistant model IC-1128GBM, however, only a few isolated positive cells were seen until day 7 (Fig. 3A, e–h).

To determine whether SVV-001 infects normal mouse brain cells, the whole mouse brain on IHC stained paraffin sections was examined as we described previously.[33] Similar to our previous observations in medulloblastoma xenograft mouse models,[33] SVV-001 did not infect any adjacent cerebellar granular neurons in ICb-1277AA (Fig. 3B, i–k). Viral capsid proteins were also absent in the ventricles, glial cells, or cells in the cerebral gray or white matter (Fig. 3B, n), indicating that SVV-001 spared normal mouse brain cells.

SVV-001 Prolongs Animal Survival Times In vivo

To evaluate the therapeutic efficacy of SVV-001 and gain a better understanding of intertumoral heterogeneity, we treated 3 permissive mouse models identified from the in vitro studies with single tail vein injection of SVV-001 (5×10^{12} vp/kg). An additional 2 resistant GBM models were also included to correlate their in vivo responses with in vitro sensitivities. To further determine the impact of tumor size on responses toward SVV-001, we divided the treated mice into 2 groups. For the small tumor group, the single tail vein injection of SVV-001 was performed 2 weeks post tumor cell transplantation when the xenograft tumors were <1 mm in size as estimated on serial sections of mouse brains; and for the medium tumor group, the treatment was delayed until the fourth week, when the xenografts were 1–4 mm in size. Compared with the control group that received the placebo treatment, significant extension of animal survival times was observed in all 3 permissive models ($P < .01$; Fig. 4A and B). In ICb-1227AA, animal survival times were prolonged from 59.1 ± 1.2 days in the control group to 127 ± 28 days (116.1%, $P < .001$) in the small tumor group and to 241 ± 31 days (307.9%, $P < .001$) in the medium tumor group. From the serial paraffin sections of the whole mouse brains of the long-term survivors in ICb-1227AA, complete elimination of xenograft tumors was found in 2 (20%) and 8 (80%) of the 10 mice that were treated at 2 weeks and 4 weeks, respectively, after tumor injections (Fig. 4C). In IC-1406GBM, the animal survival time in both the small and medium tumor groups increased 57% from 73 ± 6.5 to 115.1 ± 7 and 115.9 ± 9 days ($P < .001$), respectively. In IC-1621GBM, animal survival times increased 18% and 33.8% ($P = .007$), respectively. When the effects of SVV-001 on small tumor groups were compared with those on the medium groups, no significant differences ($P < .05$) were observed in IC-1406GBM and IC-1621GBM, whereas in the third model (IC-1227AA), mice bearing medium-sized tumors at time of treatment survived significantly longer ($P < .01$) than those with small tumors. In the 2 resistant mouse models that did not respond to SVV-001 in vitro, no survival benefit was observed in IC-1128GBM ($P > .05$), whereas in

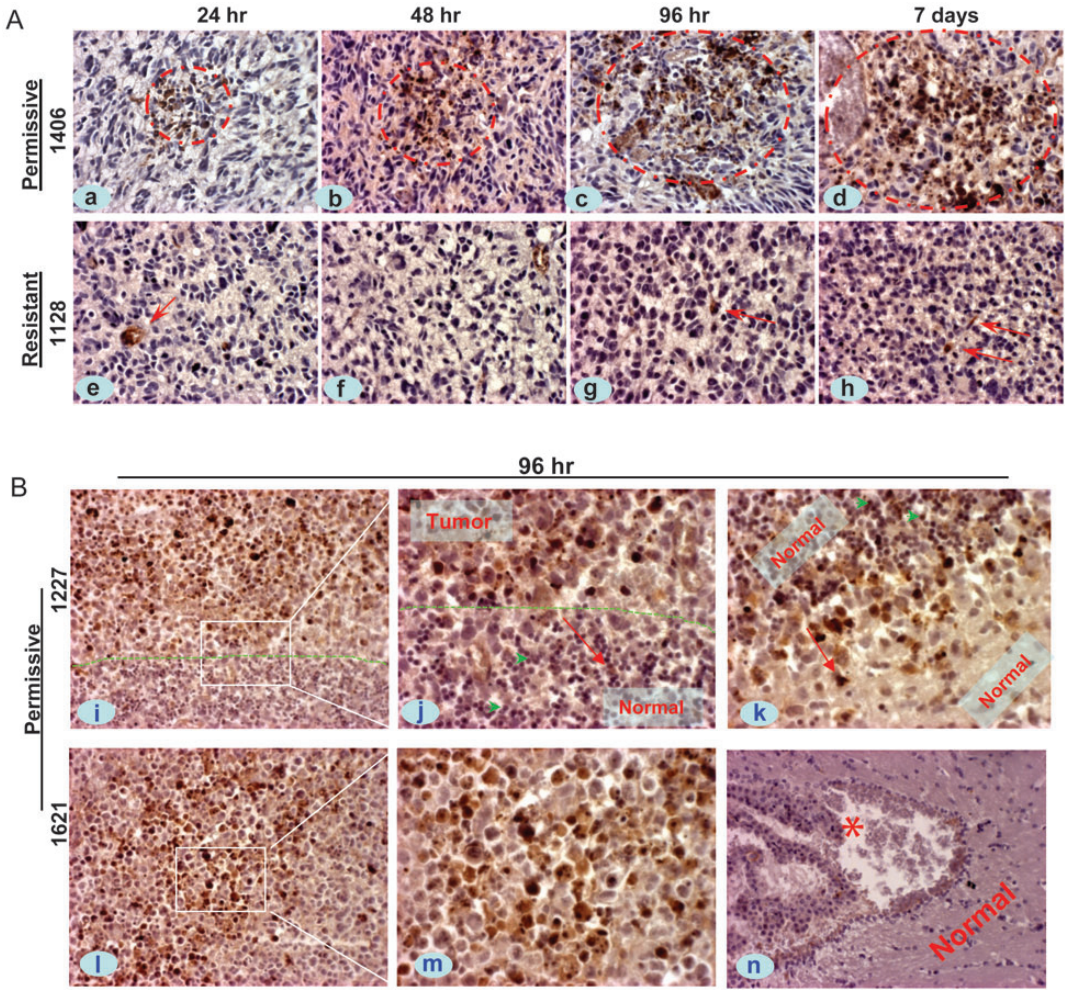

Fig. 3. In vivo infection of SVV-001 in the orthotopic xenograft tumors of pediatric GBM. Mice bearing relatively large intracerebral xenografts (8–10 wk post tumor cell transplantation) received a single tail vein injection of SVV-001 (5×10^{12}vp/kg), after which whole brains were removed at predetermined time points (24 h to 7 days), followed by IHC staining using antibodies specific to the capsid proteins of SVV-001. (A) Representative images showing the time-course increase of positively infected xenograft cells (circled in red) in the permissive model IC-1406GBM (1406, a–d), as contrast to the isolated positive reactions (arrow) in the resistant model IC-1128GBM (1128, e–h). (B) IHC staining of SVV-001 capsid protein in 2 additional permissive models, ICb-1227AA (1227, i–k) and IC-1621GBM (1621, l–m), 96 h post virus injection. The "border" between tumor mass and normal mouse brain in ICb-1277AA is marked by dotted lines (i and j). SVV-001–infected tumor cells both in the core area (i, l–m) and in the invasive front (i–k), including the single invasive cells (j and k, arrow); while sparing the normal mouse granular neurons that are in close proximity with the tumor cells in ICb-1227AA (j, green arrowhead). No SVV-001 positivity was detected in the left ventricle (*) and normal cerebral tissue (n) despite strong positive reaction in tumor cells (l–m) in the same mouse brain of IC-1621GBM. Red arrows in j and k also mark the direction of tumor cell migration. Magnification: ×40 (a–h, j, k, m), ×20 (i, l, n).

IC-1520GBM, SVV-001 was able to prolong the survival of mice bearing medium-sized tumors from 86.8 ± 9.7 days to 114.8 ± 8.9 days (32% increase, $P = .002$), suggesting that some discrepancies still exist between in vitro and in vivo assays. Based on the in vivo efficacy, IC-1502GBM was re-classified as permissive (Fig. 4A).

Intravenously Injected SVV-001 Works Better in Tumors With Well-developed Blood Vessels

It is well established that cancer drugs work better with reduced tumor burden. Since medium-sized tumors in the IC-1227AA group responded better than the small tumors, we thought the differences of blood supply between the medium and the small tumors might have played a role. Examination of hematoxylin and eosin–stained serial paraffin sections of whole mouse brains showed that indeed the microxenograft tumors were composed of 100–200 cells in the 2-week group, much smaller than in the 4-week group (~1.5 mm) (Fig. 5A, a, b). The microvessel density, estimated by examining the number of blood vessels that contained <8 red blood cells on 5 high-power fields (Fig. 5A), was 1.2 ± 1.05 in the 2-week group and 8.6 ± 0.89 in the 4-week group ($P < .001$; Fig. 5B), suggesting that poor blood supply to the micronodules may have impeded

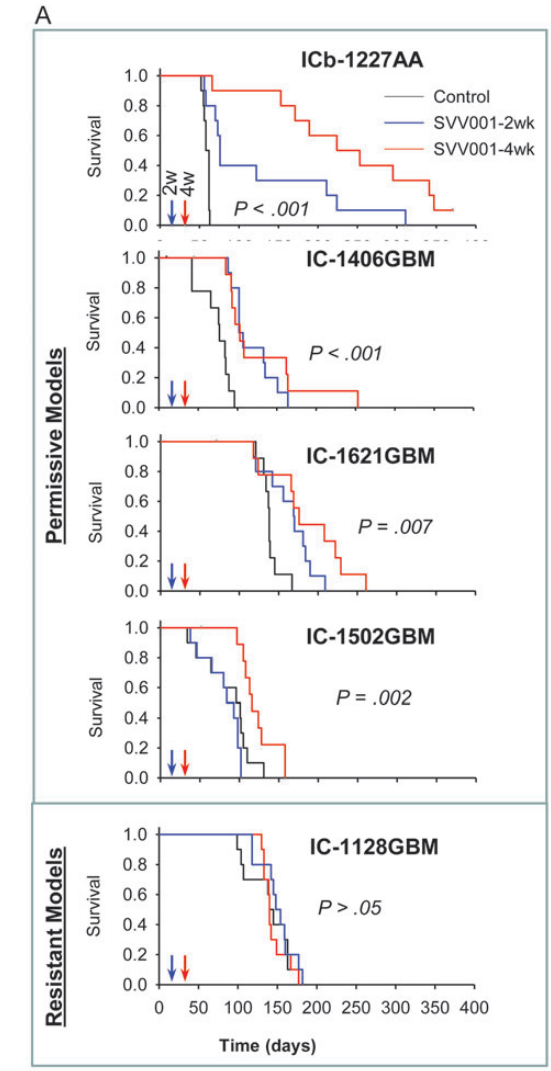

B

Pair-wise multiple comparisons between control and the treated (2 wk and 4 wk) groups.

Models	Untreated v.s. 2 wk	Untreated v.s. 4 wk	2 wk v.s. 4 wk
ICb-1227AA	Yes	Yes	Yes
IC-1406GBM	Yes	Yes	No
IC-1621GBM	Yes	Yes	No
IC-1502GBM	No	Yes	Yes
IC-1128GBM	No	No	No

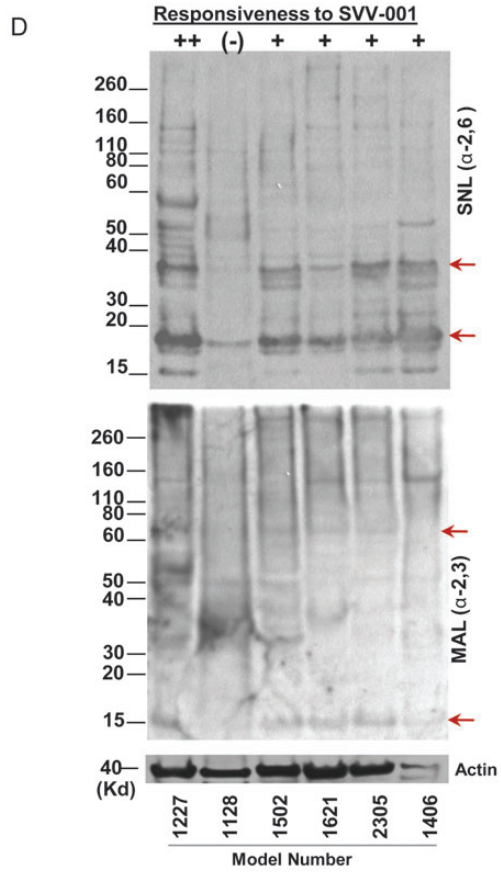

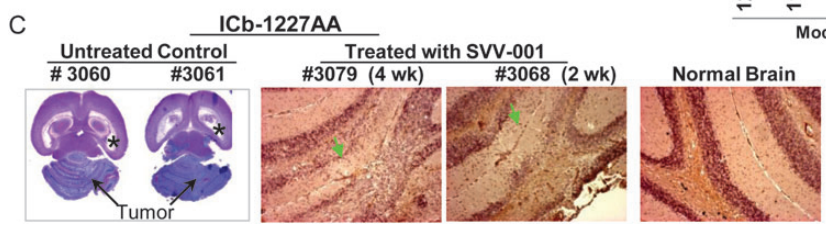

Fig. 4. Systemic treatment of preformed GBM xenograft tumors with SVV-001 significantly prolongs survival times. (A) Graphs showing the log-rank analysis of animal survival times. Treatment of preestablished orthotopic xenografts ($n = 10$ per group) was performed through a single tail vein injection of SVV-001 (5×10^{12}vp/kg) after the engrafted tumor cells (1×10^{5}/mouse) were allowed to grow for 2 and 4 wk, respectively. Mice in the control group ($n = 10$) received the injection of PBS that was used to resuspend SVV-001. (B) All pairwise multiple comparison procedures were performed with the Holm–Sidak method to isolate the group or groups that differ from the others. (C) Representative images showing the elimination of ICb-1227AA xenografts by SVV-001. In the untreated animals (#3060 and #3061), the growth of xenograft tumors (arrows) almost completely destroyed the mouse cerebellum and caused severe hydrocephalus, as evidenced by enlarged bilateral ventricles (*). In the 2 mice that were treated with SVV-001 4 wk (#3079) and 2 wk (#3068) post tumor injection, respectively, no remnant of human tumor cells were detected with IHC staining using human-specific monoclonal antibodies against mitochondria, although disturbances of granular layer caused by surgical procedure were visible (arrow) compared with normal brain. (D) Western hybridization showing the decreased content of α2,6-linked (top panel) α2,3-linked (middle panel) sialic acids in the resistant model IC-1128GBM (1128) compared with the 5 permissiveness models (++ to +) toward SVV-001 in vivo and/or in vitro. Biotinylated lectins SNL (for α2,6-linkage) and MAL (for α2,3-linkage) were applied to proteins extracted from the xenograft tumors. Arrows indicate the bands that were missing or significantly reduced in the resistant model (IC-1128GBM).

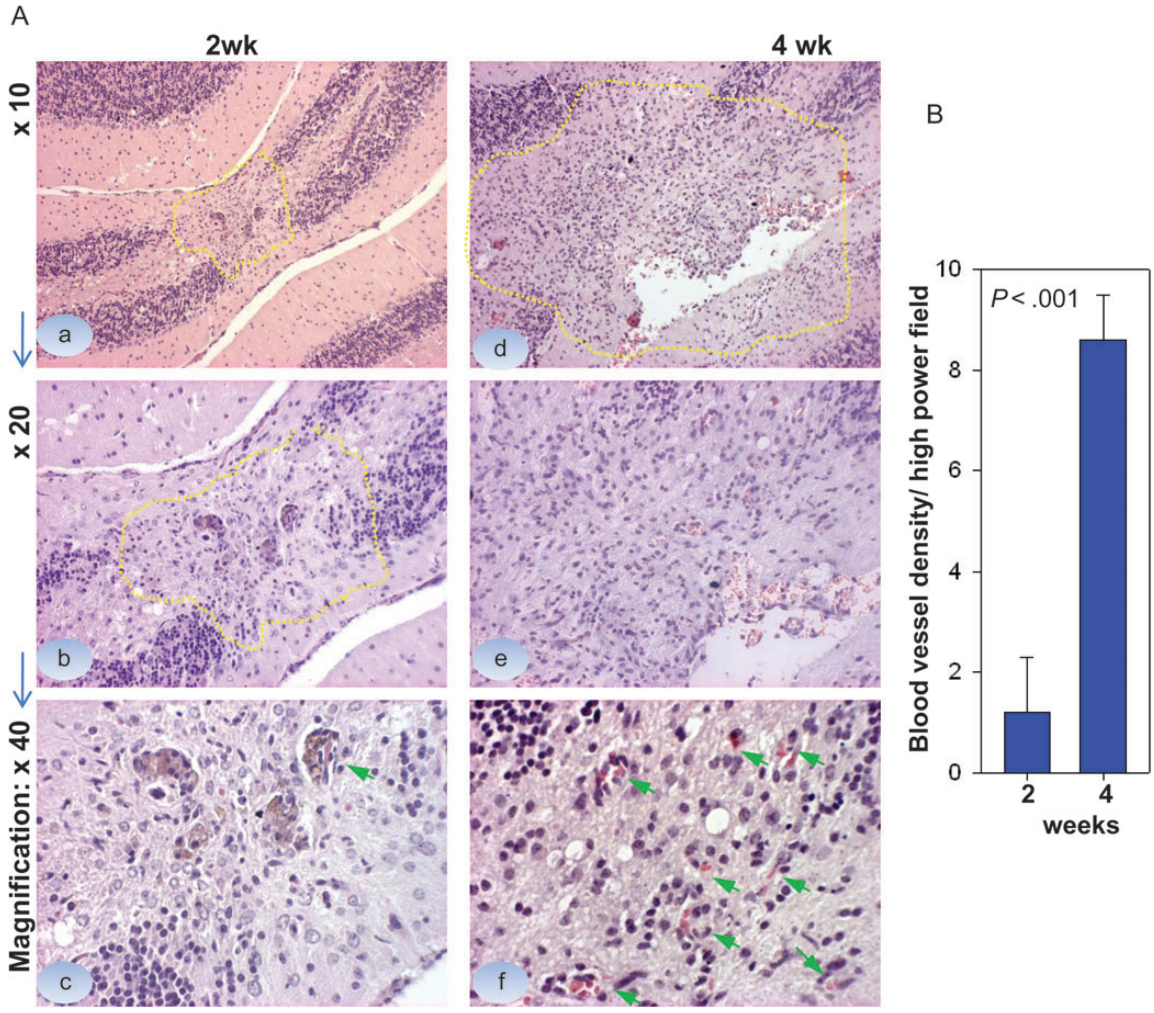

Fig. 5. Comparison of microvessel density between the small and the medium-sized xenograft tumors in IC-1227AA. (A) Representative images showing the overall sizes of xenograft tumors 2 wk (a, b) and 4 wk (d, e) post tumor cell injection. Microvessel density was estimated by counting the intratumoral blood vessels containing <8 red blood cells under high power (×40) magnifications (c, d, arrows). (B) Graph showing the significantly lower density of blood vessels in the 2-wk tumors compared with the 4-wk tumors ($P < .001$).

the access of i.v. injected SVV-001 viruses to the tumor cells.

Permissiveness of GBM Xenograft Tumors Was Correlated With Their Sialic Acid Contents

Because not all GBM responds equally to SVV-001, it is highly desired to identify diagnostic marker(s) that will help differentiate the permissive from the resistant tumors. Multiple RNA viruses, including members of *Picornaviridae*, use sialic acid as a component of their cellular receptor.[37,45] Because SVV-001 did not infect any of the 13 normal human cells, including fetal astrocyte and neural cells,[28] we reasoned that the aberrant changes of sialic acid in human cancer cells might contribute to the selective tumor cell tropism of SVV-001. To examine whether the sialic acid level of GBM xenografts correlated with their permissiveness, we performed Western hybridization in 5 permissive mouse models and 1 resistant model (IC-1128GBM) using 2 biotinylated lectins, SNL and MAL, which bind preferentially to α2,6-linked and α2,3-linked sialic acids, respectively. In the permissive models, multiple bands were detected by SNL and MAL, indicating that α2,6-linked and α2,3-linked sialic acids were present in different proteins. Worthy of note is that the 2 most responsive tumors, in ICb-1277AA and IC-1406GBM, appeared to have relatively higher levels of SNL (Fig. 4D, upper panel). In contrast, the overall levels of sialic acids were much lower in the resistant model, IC-1128GBM; and at least 2 brands that were present in the permissive models were missing or significantly reduced in the resistant model (Fig. 4D).

SVV-GFP Infection of GBM Cells Requires Sialic Acid

To functionally determine whether sialic acid is required for SVV-GFP infection, GBM cells from 2 permissive mouse models, IC-1406GBM and IC-2305GBM, were treated with *V. cholerae* neuraminidase, which cleaves

α2,3-linked and α2,6-linked terminal sialic acid residues and α2,8-linked internal sialic acid residues, and we examined the changes of SVV-GFP infectivity (Fig. 6). Although high doses of neuraminidase (>25 mM/mL) caused some suppression of cell proliferation (Fig. 6A), the infectivity of SVV-GFP in the viable cells of IC-1406GBM was reduced to 58% by 3.125 mU/mL neuraminidase and to 40% by 25 mU/mL

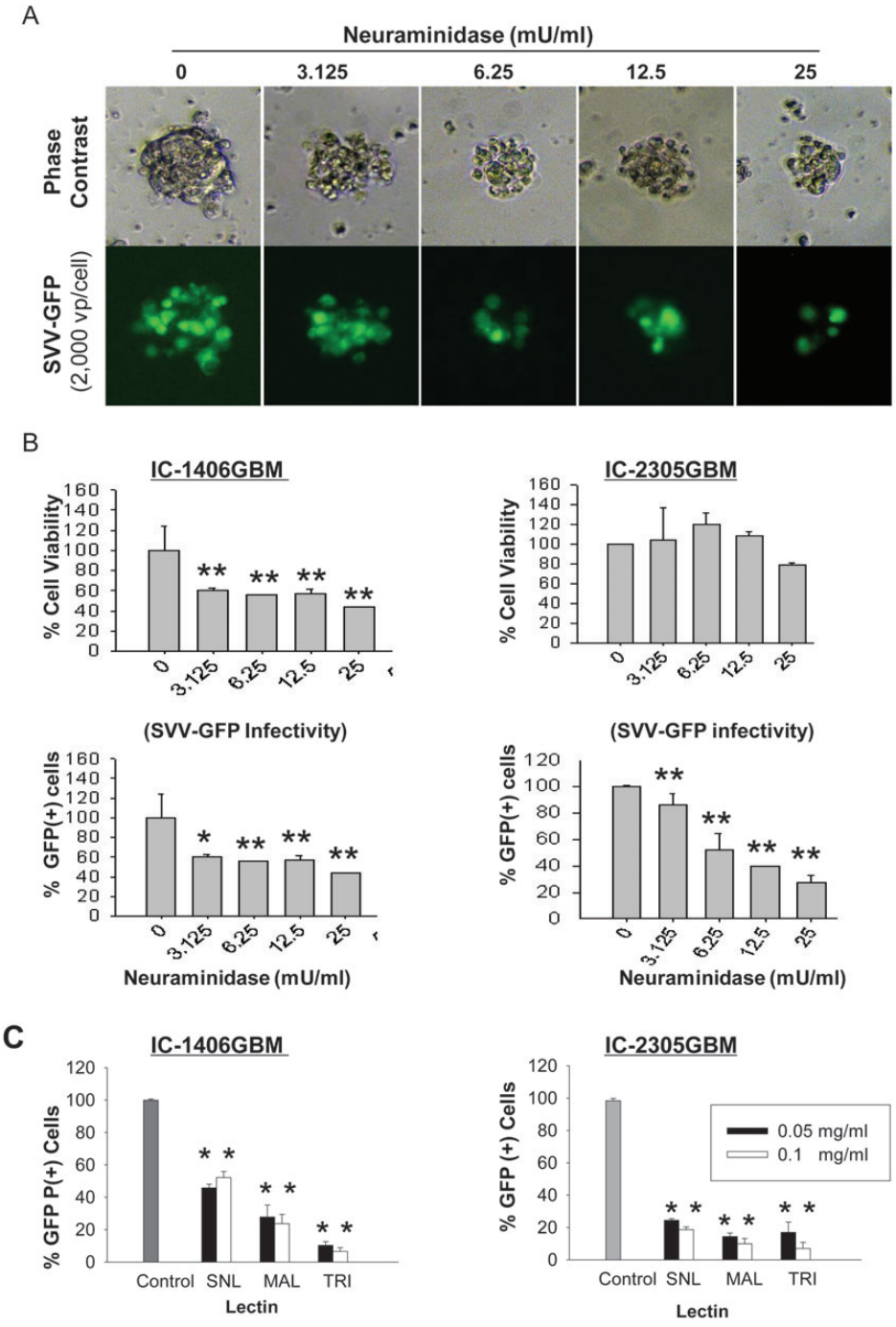

Fig. 6. Infection of SVV-GFP in pediatric gliomas is mediated through the binding of sialic acid. (A) Representative images showing the dose-dependent suppression of SVV-GFP infection by neuraminidases, which cleave α2,3-linked and α2,6-linked terminal sialic acid residues and α2,8-linked internal sialic acid residues, in neurospheres derived from IC-1406GBM. (B) Quantitative analysis of the changes of cell viability (top panel) and the infectivity of SVV-GFP (lower panel) in pediatric GBM by treating 2 preformed neurospheres in quadruplicates with neuraminidase. Results in the treated cells were normalized to those of the untreated control. $*P < .05$, $**P < .01$. (C) Inhibition of SVV-GFP infection by linkage-specific lectins. SNL binds preferentially to α2,6-linked sialic acid, MAL to α2,3-linked sialic acid, and TRI to both α2,6-linked and α2,3-linked acids. Significant suppression was caused by all 3 lectins in the 2 models compared with untreated control ($**P < .01$).

neuraminidase. In IC-2305GBM cells, the infectivity of SVV-GFP was significantly reduced to 50% with 6.25 mM/mL and further down to 25% with 25 mM/mL neuraminidase in the viable cells ($P < .05$; Fig. 6B). These data suggest that sialic acid played a role in mediating SVV-GFP infectivity and that xenograft tumor cells derived from different patients were not equally sensitive to the neuraminidase treatment.

Both α2,3-linked and α2,6-linked Sialic Acids Were Involved in SVV-GFP Infection

To further identify the specific linkage of sialic acid that mediates SVV-GFP infection, we used MAL, which binds preferentially to α2,3-linked sialic acid, and SNL, which binds preferentially to α2,6-linked sialic acid, to block the potential binding sites of SVV-GFP. As shown in Fig. 5C, pre-incubation of IC-1406GBM and IC-2305GBM cells for 1 h with SNL and MAL reduced GFP^+ cells to <50% and 30%, respectively, of the control group ($P < .05$). The difference between SNL- and MAL-treated cells was significant ($P < .05$), suggesting that α2,3-linked sialic acid played a more important role than the α2,6-linked sialic acid. Increasing the lectin concentration from 0.05 mg/mL to 0.1 mg/mL did not cause further suppression of SVV-GFP infection in IC-1406GBM, indicating that 0.05 mg/mL is sufficient to block most, if not all, of the binding sites of SVV-GFP in sialic acids. In IC-2305GBM cells, high doses of lectins resulted in slightly lower infection, but a significant difference ($P < .05$) was found in only SNL-treated cells.

To further examine whether simultaneous blocking of both α2,3- and α2,6-linked sialic acids would synergistically suppress SVV-GFP infection, we pretreated the tumor cells with TRI, which binds to both α2,3- and α2,6-linked sialic acids. As shown in Fig. 6C, a 1-h pretreatment with TRI further reduced the GFP^+ cells to <10% in IC-1406GBM, much lower than that achieved by competitively blocking α2,3- or α2,6-linked sialic acid alone ($P < .05$). In IC-2305GBM, significant differences were observed between cells treated with higher concentrations (0.1 mg/mL) of TRI and SNL ($P < .05$) but not between TRI and MAL. Altogether, these results suggest that both α2,3- and α2,6-linked sialic acids are involved in mediating the infection of SVV-001 in pediatric GBM.

Discussion

We show here for the first time that the oncolytic picornavirus SVV-001 possesses significant antitumor activities against pediatric malignant gliomas. We demonstrated that SVV-001 can effectively kill primary cultured glioma xenograft cells in 4 of the 6 models that were directly derived from patient tumors. We also showed that SVV-001 can infect the pre-established GBM neurospheres and kill self-renewing single GBM cells in vitro. More importantly, we demonstrated that systemically administered SVV-001 via a single i.v. injection can pass through the BBB, penetrate into orthotopic xenografts, and infect glioma cells without harming normal mouse cells, leading to significant prolongation of animal survival times in all 3 of the permissive mouse models. Mechanistically, we identified α2,3- and α2,6-sialic acids as key mediators of SVV-001 infection in glioma cells.

Due to the lack of in vitro and in vivo model systems, few new therapies are tested in vitro and in vivo for pediatric malignant gliomas. The 6 primary tumor-based orthotopic xenograft mouse models, the first and the largest panel that have been reported so far, have thus provided us with a unique opportunity to perform rigorous preclinical studies to determine the therapeutic efficacy of SVV-001 in a setting that is close to human tumors. Since all of our models are patient-specific and represent the heterogeneous nature of pediatric GBM, our observed variability in response will help to estimate the patient response rate in pediatric gliomas to SVV-001. Our identification of 4 (66.7%) permissive tumors from the 6 models suggests that more than half of children with malignant gliomas can potentially benefit from SVV-001 treatment. More importantly, we showed that SVV-001 acting as a single agent was able to eliminate orthotopic xenograft tumors in 2 (20%) and 8 (80%) of the IC-1227AA mice treated at 2 and 4 weeks, respectively, after tumor cell injections. We also noted that very small xenograft tumors with poorly developed intratumoral blood vessels were less responsive than larger tumors with rich blood vessels in IC-1227AA. Failure to eradicate the preformed xenograft tumors in the remaining permissive models suggested that there still existed some SVV-001–resistant tumor cells even within the permissive models. Since combining adenovirus with radiation has increased efficacy in adult GBM,[46] it may be worth the effort to examine whether combining radiation or chemotherapy with SVV-001 would further enhance the efficacy in pediatric GBM as well.

Development of diagnostic marker that can differentiate permissive from resistant gliomas is important for patient stratification in future clinical trials and applications of SVV-001. Previous virological studies indicate that binding to target cell receptors is a critical initiating step in the virus life cycle.[34] Sialic acids are shown to be used by a number of viruses as a component of their cellular receptors and may lead to restrictions in host range, tissue tropism, and pathogenesis/oncolytic activities.[37] An example of this can be seen by the preference of avian influenza for α2,3-linked sialic acid and growth of this virus in intestinal cells in birds, whilst human influenza uses α2,6-linked sialic acid and grows in cells of the respiratory tract.[47,48] In this study, we found that the contents of sialic acids correlated with the permissiveness of GBM xenograft tumors toward SVV-001 with Western hybridization and identified several missing bands in the resistant model IC-1128GBM. Although future studies are needed to identify the backbone proteins, our subsequent studies confirmed the role of sialic acid in SVV-001 infection of GBM cells using linkage-specific neuraminidase and lectins. Unlike many viruses that bind to sialic acid via 1 specific glycosidic linkage, mostly the α2,3 link,[49,50] our data indicated that SVV-001 binds to both α2,3- and α2,6-linked sialic

acids, as simultaneous blocking of both sialic acids resulted in synergistic inhibition of SVV-GFP infection that was stronger than blocking either one alone. This result suggests that the attachment of SVV-001 to pediatric GBM cells may be dependent on a complex structure using more than 1 sialic acid residue, which warrants further experiments to determine whether the sialic acid residues are located on a carbohydrate complex, glycoproteins, or glycolipids. Since sialic acids are widely present in various normal cells, and previous studies have shown that none of the 13 normal primary human cells were infected when exposed to high MOI (>10 000 vp/cell),[28] our data suggest that the altered backbone structure (protein, glycolipids, or carbohydrate complex) of sialic acid, as a result of genetic abnormalities that occurred in pediatric gliomas, might have played an important role in granting their permissiveness to SVV-001.

Both the innate and acquired immune systems may dramatically modulate oncolytic efficacy. In fact, it has been reported that innate antiviral immune responses were one of the major barriers to effective oncolytic myxoma virus virotherapy in adult glioma.[16] Because our study was conducted in SCID (immune-deficient) mice, we were not able to examine the impact of the host immune response on the infection and cell killing of pediatric GBM. Although some other studies also suggested that host immune mechanisms may contribute to tumor eradication following administration of oncolytic viruses,[51] a detailed evaluation of SVV-001 in an immune-competent tumor model as described recently with the herpes simplex virus[52] will help to fully elucidate the role of immune responses in its antitumor activities.

In summary, our results demonstrated the potent antitumor activities of SVV-001 against pediatric gliomas. Because this study was performed in a relatively large panel of primary tumor–based orthotopic xenograft models, it provided a preclinical rationale that supports the consideration of SVV-001 for clinical trials against pediatric anaplastic astrocytoma and GBM. Our results also identified the α2,3- and α2,6-linked sialic acids as key components that mediate SVV-001 infection, which represents an important first step for future identification of SVV-001 receptors that can potentially be used as diagnostic markers in pediatric GBM.

Supplementary Material

Supplementary material is available online at *Neuro-Oncology* (http://neuro-oncology.oxfordjournals.org/).

Acknowledgments

The authors acknowledge the joint participation by the Diana Helis Henry Medical Research Foundation through it's direct engagement in the continuous active conduct of medical research in conjunction with Baylor College of Medicine and the Eliminating Brain Tumor Stem Cells with an Oncolytic Picornavirus Program.

Conflict of interest statement. N.I., S.R.P., and P.L.H. were employees of Neotropix. No conflicts exist for the remaining authors.

References

1. Glas M, Happold C, Rieger J, et al. Long-term survival of patients with glioblastoma treated with radiotherapy and lomustine plus temozolomide. *J Clin Oncol*. 2009;27:1257–1261.
2. Shih CS, Hale GA, Gronewold L, et al. High-dose chemotherapy with autologous stem cell rescue for children with recurrent malignant brain tumors. *Cancer*. 2008;112:1345–1353.
3. Diehn M, Cho RW, Clarke MF. Therapeutic implications of the cancer stem cell hypothesis. *Semin Radiat Oncol*. 2009;19:78–86.
4. Bao S, Wu Q, McLendon RE, et al. Glioma stem cells promote radioresistance by preferential activation of the DNA damage response. *Nature*. 2006;444:756–760.
5. Hemmati HD, Nakano I, Lazareff JA, et al. Cancerous stem cells can arise from pediatric brain tumors. *Proc Natl Acad Sci U S A*. 2003;100:15178–15183.
6. Chen R, Nishimura MC, Bumbaca SM, et al. A hierarchy of self-renewing tumor-initiating cell types in glioblastoma. *Cancer Cell*. 2010;17:362–375.
7. Schatton T, Murphy GF, Frank NY, et al. Identification of cells initiating human melanomas. *Nature*. 2008;451:345–349.
8. Cripe TP, Wang PY, Marcato P, Mahller YY, Lee PW. Targeting cancer-initiating cells with oncolytic viruses. *Mol Ther*. 2009;17:1677–1682.
9. Everson RG, Gromeier M, Sampson JH. Viruses in the treatment of malignant glioma. *Expert Rev Neurother*. 2007;7:321–324.
10. Studebaker AW, Hutzen B, Pierson CR, et al. Oncolytic measles virus prolongs survival in a murine model of cerebral spinal fluid-disseminated medulloblastoma. *Neuro Oncol*. 2012;14:459–470.
11. Sonabend AM, Ulasov IV, Han Y, Lesniak MS. Oncolytic adenoviral therapy for glioblastoma multiforme. *Neurosurg Focus*. 2006;20:E19.
12. Jiang H, Gomez-Manzano C, Lang FF, Alemany R, Fueyo J. Oncolytic adenovirus: preclinical and clinical studies in patients with human malignant gliomas. *Curr Gene Ther*. 2009;9:422–427.
13. Wilcox ME, Yang W, Senger D, et al. Reovirus as an oncolytic agent against experimental human malignant gliomas. *J Natl Cancer Inst*. 2001;93:903–912.
14. Lun X, Senger DL, Alain T, et al. Effects of intravenously administered recombinant vesicular stomatitis virus (VSV(deltaM51)) on multifocal and invasive gliomas. *J Natl Cancer Inst*. 2006;98:1546–1557.
15. Geletneky K, Kiprianova I, Ayache A, et al. Regression of advanced rat and human gliomas by local or systemic treatment with oncolytic parvovirus H-1 in rat models. *Neuro Oncol*. 2010;12:804–814.
16. Lun X, Alain T, Zemp FJ, et al. Myxoma virus virotherapy for glioma in immunocompetent animal models: optimizing administration routes and synergy with rapamycin. *Cancer Res*. 2010;70:598–608.
17. Zulkifli MM, Ibrahim R, Ali AM, et al. Newcastle diseases virus strain V4UPM displayed oncolytic ability against experimental human malignant glioma. *Neurol Res*. 2009;31:3–10.

18. Dobrikova EY, Broadt T, Poiley-Nelson J, et al. Recombinant oncolytic poliovirus eliminates glioma in vivo without genetic adaptation to a pathogenic phenotype. *Mol Ther*. 2008;16:1865–1872.
19. Heikkila JE, Vaha-Koskela MJ, Ruotsalainen JJ, et al. Intravenously administered alphavirus vector VA7 eradicates orthotopic human glioma xenografts in nude mice. *PLoS One*. 2010;5:e8603.
20. Jiang H, Gomez-Manzano C, Aoki H, et al. Examination of the therapeutic potential of delta-24-RGD in brain tumor stem cells: role of autophagic cell death. *J Natl Cancer Inst*. 2007;99:1410–1414.
21. Wakimoto H, Kesari S, Farrell CJ, et al. Human glioblastoma-derived cancer stem cells: establishment of invasive glioma models and treatment with oncolytic herpes simplex virus vectors. *Cancer Res*. 2009;69:3472–3481.
22. Friedman GK, Langford CP, Coleman JM, et al. Engineered herpes simplex viruses efficiently infect and kill CD133+ human glioma xenograft cells that express CD111. *J Neurooncol*. 2009;95:199–209.
23. Skog J, Edlund K, Bergenheim AT, Wadell G. Adenoviruses 16 and CV23 efficiently transduce human low-passage brain tumor and cancer stem cells. *Mol Ther*. 2007;15:2140–2145.
24. Tyler MA, Ulasov IV, Sonabend AM, et al. Neural stem cells target intracranial glioma to deliver an oncolytic adenovirus in vivo. *Gene Ther*. 2008;16:262–278.
25. Myers R, Harvey M, Kaufmann TJ, et al. Toxicology study of repeat intracerebral administration of a measles virus derivative producing carcinoembryonic antigen in rhesus macaques in support of a phase I/II clinical trial for patients with recurrent gliomas. *Hum Gene Ther*. 2008;19:690–698.
26. Lun XQ, Jang JH, Tang N, et al. Efficacy of systemically administered oncolytic vaccinia virotherapy for malignant gliomas is enhanced by combination therapy with rapamycin or cyclophosphamide. *Clin Cancer Res*. 2009;15:2777–2788.
27. Yong RL, Shinojima N, Fueyo J, et al. Human bone marrow–derived mesenchymal stem cells for intravascular delivery of oncolytic adenovirus delta24-RGD to human gliomas. *Cancer Res*. 2009;69:8932–8940.
28. Reddy PS, Burroughs KD, Hales LM, et al. Seneca Valley virus, a systemically deliverable oncolytic picornavirus, and the treatment of neuroendocrine cancers. *J Natl Cancer Inst*. 2007;99:1623–1633.
29. Venkataraman S, Reddy SP, Loo J, et al. Crystallization and preliminary x-ray diffraction studies of Seneca Valley virus–001, a new member of the *Picornaviridae* family. *Acta Crystallogr Sect F Struct Biol Cryst Commun*. 2008;64:293–296.
30. Wadhwa L, Hurwitz MY, Chevez-Barrios P, Hurwitz RL. Treatment of invasive retinoblastoma in a murine model using an oncolytic picornavirus. *Cancer Res*. 2007;67:10653–10656.
31. Morton CL, Houghton PJ, Kolb EA, et al. Initial testing of the replication competent Seneca Valley virus (NTX-010) by the pediatric preclinical testing program. *Pediatr Blood Cancer*. 2010;55:295–303.
32. Rudin CM, Poirier JT, Senzer NN, et al. Phase I clinical study of Seneca Valley virus (SVV-001), a replication-competent picornavirus, in advanced solid tumors with neuroendocrine features. *Clin Cancer Res*. 2011;17:888–895.
33. Yu L, Baxter PA, Zhao X, et al. A single intravenous injection of oncolytic picornavirus SVV-001 eliminates medulloblastomas in primary tumor-based orthotopic xenograft mouse models. *Neuro Oncol*. 2010;13:14–27.
34. Campbell SA, Gromeier M. Oncolytic viruses for cancer therapy I. Cell-external factors: virus entry and receptor interaction. *Onkologie*. 2005;28:144–149.
35. Nilsson EC, Jamshidi F, Johansson SM, Oberste MS, Arnberg N. Sialic acid is a cellular receptor for Coxsackievirus A24 variant, an emerging virus with pandemic potential. *J Virol*. 2008;82:3061–3068.
36. Stevenson RA, Huang JA, Studdert MJ, Hartley CA. Sialic acid acts as a receptor for equine rhinitis A virus binding and infection. *J Gen Virol*. 2004;85:2535–2543.
37. Alexander DA, Dimock K. Sialic acid functions in enterovirus 70 binding and infection. *J Virol*. 2002;76:11265–11272.
38. Houghton PJ, Adamson PC, Blaney S, et al. Testing of new agents in childhood cancer preclinical models: meeting summary. *Clin Cancer Res*. 2002;8:3646–3657.
39. Shu Q, Wong KK, Su JM, et al. Direct orthotopic transplantation of fresh surgical specimen preserves CD133+ tumor cells in clinically relevant mouse models of medulloblastoma and glioma. *Stem Cells*. 2008;26:1414–1424.
40. Li XN, Shu Q, Su JM, et al. Valproic acid induces growth arrest, apoptosis, and senescence in medulloblastomas by increasing histone hyperacetylation and regulating expression of p21Cip1, CDK4, and CMYC. *Mol Cancer Ther*. 2005;4:1912–1922.
41. Lee J, Kotliarova S, Kotliarov Y, et al. Tumor stem cells derived from glioblastomas cultured in bFGF and EGF more closely mirror the phenotype and genotype of primary tumors than do serum-cultured cell lines. *Cancer Cell*. 2006;9:391–403.
42. Shu Q, Antalffy B, Su JM, et al. Valproic acid prolongs survival time of severe combined immunodeficient mice bearing intracerebellar orthotopic medulloblastoma xenografts. *Clin Cancer Res*. 2006;12:4687–4694.
43. Hales LM, Knowles NJ, Reddy PS, et al. Complete genome sequence analysis of Seneca Valley virus–001, a novel oncolytic picornavirus. *J Gen Virol*. 2008;89:1265–1275.
44. Chaichana K, Zamora-Berridi G, Camara-Quintana J, Quinones-Hinojosa A. Neurosphere assays: growth factors and hormone differences in tumor and nontumor studies. *Stem Cells*. 2006;24:2851–2857.
45. Zhou L, Luo Y, Wu Y, Tsao J, Luo M. Sialylation of the host receptor may modulate entry of demyelinating persistent Theiler's virus. *J Virol*. 2000;74:1477–1485.
46. Bieler A, Mantwill K, Holzmuller R, et al. Impact of radiation therapy on the oncolytic adenovirus dl520: implications on the treatment of glioblastoma. *Radiother Oncol*. 2008;86:419–427.
47. Matrosovich MN, Matrosovich TY, Gray T, Roberts NA, Klenk HD. Neuraminidase is important for the initiation of influenza virus infection in human airway epithelium. *J Virol*. 2004;78:12665–12667.
48. Couceiro JN, Paulson JC, Baum LG. Influenza virus strains selectively recognize sialyloligosaccharides on human respiratory epithelium: the role of the host cell in selection of hemagglutinin receptor specificity. *Virus Res*. 1993;29:155–165.
49. Nokhbeh MR, Hazra S, Alexander DA, et al. Enterovirus 70 binds to different glycoconjugates containing alpha2,3-linked sialic acid on different cell lines. *J Virol*. 2005;79:7087–7094.
50. Kumlin U, Olofsson S, Dimock K, Arnberg N. Sialic acid tissue distribution and influenza virus tropism. *Influenza Other Respi Viruses*. 2008;2:147–154.
51. Hicks AM, Riedlinger G, Willingham MC, et al. Transferable anticancer innate immunity in spontaneous regression/complete resistance mice. *Proc Natl Acad Sci U S A*. 2006;103:7753–7758.
52. Redaelli M, Franceschi V, Capocefalo A, et al. Herpes simplex virus type 1 thymidine kinase-armed bovine herpesvirus type 4-based vector displays enhanced oncolytic properties in immunocompetent orthotopic syngenic mouse and rat glioma models. *Neuro Oncol*. 2012;14:288–301.